Annika Scheunemann, Claire Jacob, Andreas Bardenhagen, David Hoffmann, Philipp Würfel

Structure-system design interdependencies of hybrid-electric aircraft during conceptual design phase

Scheunemann, A., Jacob, C., Bardenhagen, A., Hoffmann, D. & Würfel, P. (2020). Structure-system design interdependencies of hybrid-electric aircraft during conceptual design phase. Aerospace Europe Conference 2020, 00618.

Paper Id.: 00618

STRUCTURE-SYSTEM DESIGN INTERDEPENDENCIES OF HYBRID-ELECTRIC AIRCRAFT DURING CONCEPTUAL DESIGN PHASE

Annika Scheunemann [1], Claire Jacob [1], Andreas Bardenhagen [1], David Hoffmann [1], Philipp Würfel [1]

[1] TU Berlin ILR Sekr. F2, Marchstr. 12-14, 10587 Berlin, Germany, Email: a.scheunemann@tu-berlin.de, c.jacob@tu-berlin.de, andreas.bardenhagen@tu-berlin.de, d.hoffmann@protonmail.com, philippwuerfel@live.de

KEYWORDS: Hybrid Aircraft, Aircraft Structures

ABSTRACT:

The electro-hybridization of aviation might bring the strongly needed decrease of fuel emissions. As the electrification cannot be evaluated with conventional methods, the TuRbo electric Aircraft Design Environment (TRADE) was funded by the EU Clean Sky JTI initiative. The consortium aims to develop a multidisciplinary design platform in order to assess the potential of hybridization on the basis of two sample aircraft. Reference [4] gives a description and evaluation of configuration 1. Configuration 2 is described in this paper. An enhanced wing structure mass calculation based on a proposal by Torenbeek is introduced and assessed. Parametric studies outline the effects of enlarged electric power and thermal systems.

1. INTRODUCTION

The growing environmental awareness calls for new configurations and propulsion systems in the aerospace sector. One step in the quest towards reaching the goals outlined in Flightpath 2050 – Europe's Vision for Aviation – could be via hybrid-electric powered aircraft [2]. The very high power demand of an electrical primary propulsion system causes an enlargement of the entire electrical system and a need for additional components, e.g. electric motors, power electronic converters, circuit breakers, generators and batteries. These enhanced electrical systems of such aircraft are much heavier and bulkier compared to the systems of today's aircraft. Their impact on structure mass and overall aircraft performance via snowball effects needs to be assessed during conceptual design phase.

The structural model, introduced in this paper, is part of the multidisciplinary design environment of advanced statistical and physics-based models. The new system components are included in the physics-based methods. An OpenMDAO frame couples the structural model with a thermal-, an electric power system-, a turbine- and a mission-model. Reference [4] provides a brief description of each model and the overall sizing process. The TRADE partners will publish more detailed descriptions and parametric studies as well as the overall results in future publications [7].

Parameter	Description	Unit
A	Area	m²
F	Force	N
M	Mass / Moment	kg / Nm
V	Velocity	m/s
b	Wing Span	m
c	Coefficient	-
f	Factor	-
k	Constant	-
n	Number	-
t	Thickness	M
x	Lever Arm	m
y	Spanwise Distance	m
σ	Normal Stress	m
Λ	Sweep Angle	°

Index	**Description**
BL	*Bending*
c	Conventional
D	Drag / Dive (Speed)
ea	Elastic Axis
EF1, EF2	Electric Fan 1, 2
eng	Engine
GT	Gas Turbine
h	Hybrid
HTP	Horizontal Tail Plane
L	Lift
Ref	Reference
rib	Rib
T	Thrust
VTP	Vertical Tail Plane

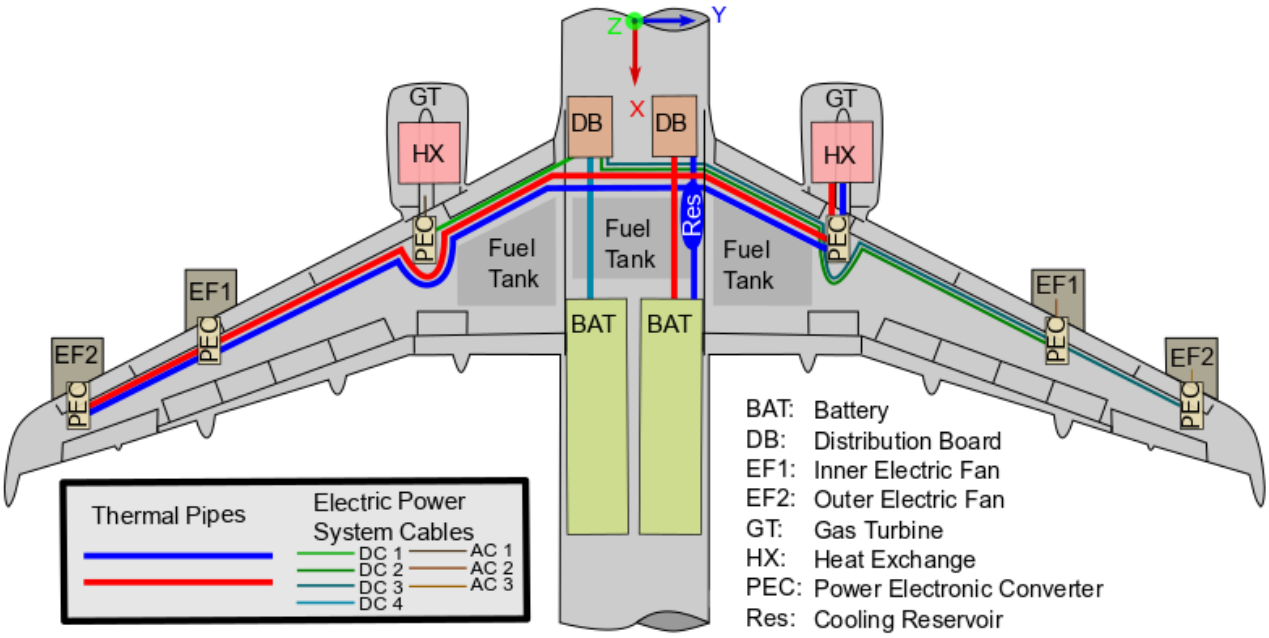

Figure 1 TRADE Configuration 2: Boosted Turbofan

2. GENERAL CONFIGURATION

The key of the configuration (TRADE configuration 2) is the "boosted turbofan" (BTF) propulsion system. It is integrated into a conventional tube-wing configuration. The design mission is to transport 150 passengers over a range of 2,500 nm. The assumed entry into service is 2035. The initial values of design parameters for sensitivity studies and later optimization will be taken from a CPACS file.

Figure 1 shows a schematic layout of the components in wing and fuselage. Two electric fans (e-fans) are connected to a gas turbine located on the opposing wing side. This layout is supposed to be advantageous in case of one-engine-inoperative (OEI). As the installations are symmetrical, for simplicity reason, the right hand side solely shows electric connections while the left wing shows thermal installations. This arrangement was elaborated in accordance with all partners, based on studies of configuration 1 in [8].

The position of fuel tanks and batteries are varied during the following studies. The model aims to find an arrangement yielding a minimal all-up mass. On the basis of two configurations, the TRADE project studies the interdependencies on the overall aircraft level.

3. SIZING OF STRUCTURAL MASS

Statistical, empirical and analytical methods are conventionally used during the conceptual and preliminary design phase in order to conduct sensitivity studies and to generate a basis for more detailed studies. These methods were developed for conventional aircraft and do not take the electric and thermal components of a BTF into account. As they offer a good resource-effort to accuracy split, they are preferred over FE based methods. Therefore, the analytical methods need to be enhanced for electro hybrid aircraft.

The statistical and empirical methods acknowledge technical improvements by technology factors (see Eq. 1).

$$M_{newTech} = M \cdot (1 - f_{technology}) \qquad (1)$$

The technology factors derive from studies conducted at the chair of Aircraft Design and Aerostructures. Table 3 lists the factors used within this study.

The model is based on following premises:

- The fuselage is designed to carry loads, no matter whether these are caused by

payloads or systems. Thus, empirical methods are presumed to be applicable.

- The electric fans, gas turbines, power electric converters and heat exchangers are located in and on the wings. An analytic method is extended to reflect the mass of systems.
- The tail is scaled according to Torenbeek [5]. The vertical tail plane is scaled to cope with the forces occurring during an OEI incident.

Table 3 Applied Technology Factors

Technology factor	Value	Reason
Tail	0.15	New Material
Fuselage	0.12	New Material
Electrical System	0.15	New Material
Air Conditioning	0.15	New Material
Galleys	0.15	New Material
Oxygen System	0.1	New Material
Emergency System	0.15	New Material

3.1. Fuselage

Torenbeek offers a statistics-based approach for the fuselage mass in [5]. As the materials defined in the CPACS files are aluminum alloys, the method yields sufficient accuracy.

3.2. Wing

The wing is categorized into primary and secondary structure. The wing box as the primary structure carries the loads, introducing them through the root into the fuselage. It consists of ribs, spars, spar webs and stiffened skin panels. The secondary structure includes high lift devices, spoilers and other control surfaces. The mass calculation reflects this separation.

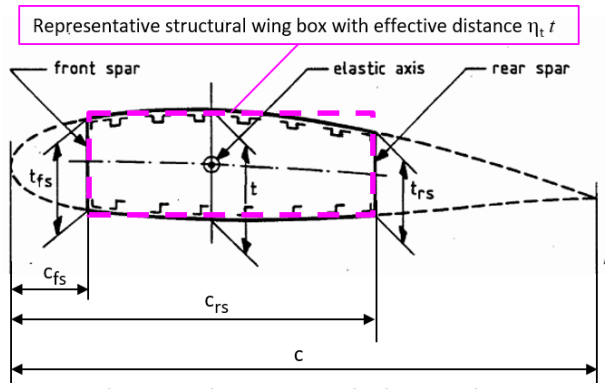

Figure 2 Wing Structure in the x-z-Plane

The wing box is positioned between front and rear spar at three characteristic wing sections: a) root, b) kink and c) tip. It is shown in Figure 2 for a typical wing section (wing profile). For each of these wing sections the relative position of front spar and rear spar are derived from the CPACS file and associated with wingspan and chord, respectively.

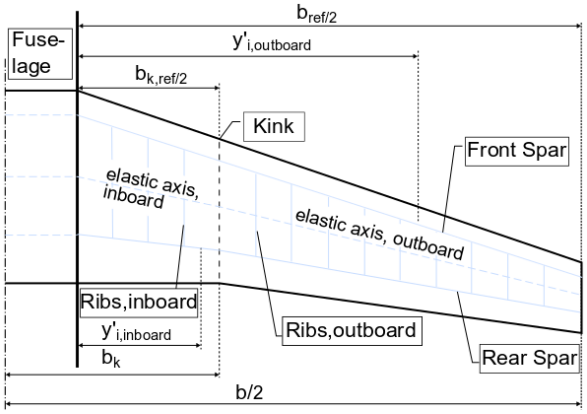

Figure 3 Wing Structure in the x-y-Plane

The slender primary structure makes it possible to use an enhanced method of the bending beam theory by Torenbeek in [6]. While Torenbeek uses an analytic approach to determine the wing mass based on bending stresses, the enhanced method uses a numeric approach calculating the stresses at each rib position. This allows to consider local load relief resulting from structure and system component mass (e.g. cables, batteries). Therefore, this enhanced method reflects the influence of the components caused by hybridization. The TRADE consortium partners Nottingham University and Mälardalen University provide the necessary masses and dimensions of the electrical and thermal system.

The wing area, sweep, aspect ratio and taper ratio are optimization parameters in the multi-disciplinary analysis and optimization (MDAO). The regression formula in Eq. 2 yields the rib amount (n_{rib}) as a function of the half wingspan (b_{ref}) between wing root and tip. The ribs are spread equidistantly between root and kink, and between kink and tip.

$$n_{rib} = 13.27 \cdot \ln(b_{ref}) - 11.77 \qquad (2)$$

Figure 3 shows the discrete model used to calculate bending moment, torsion and shear force at each rib position.

$$b_s = b_{ref} / \cos(\Lambda_{ea}) \quad (3)$$

According to [7] it can be assumed that the elastic axis of the beam is located in the middle of the wing box between front and rear spar. The beam length of the elastic axis in the wing box structure (b_s) is higher than the reference wing span due to the elastic axis sweep angle (Λ_{ea}) (Eq. 3). Therefore, a high leading edge sweep angle increases the bending moment of the wing, resulting in a higher mass of the primary structure.

Following Torenbeek's method in [6], the material necessary to resist bending, torsion and shear forces is derived from the aerodynamic loads and the lift relief due to the mass of the primary and secondary wing structure, propulsion, electrical and thermal systems.

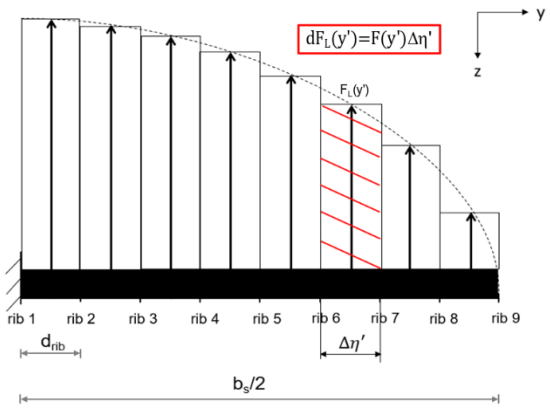

Figure 4 Lift Distribution

The aerodynamic lift is assumed to be distributed elliptically, which is sufficient for wing structure sizing (Figure 4). All aerodynamic loads and weight relief (engines, batteries, fuel, etc.) act along the elastic axis and the resulting bending moment, torsion, shear force can be calculated at each rib position. Considered load cases are derived from the flight envelope, e.g. the typical 2,5g pull-up manoeuvre.

The resulting bending moment (M_{BL}) and shear forces are calculated at each rib position. As the structural model of the wing box is a beam with a nearly rectangular cross section (Figure 2), the necessary material to resist bending is determined by

$$A(y) = \frac{M_{BL}(y)}{\eta_t \, t(y) \, |\sigma(y)|} \quad (4)$$

The material depending allowable normal stress (σ) and the effective distance ($\eta_t \cdot t$) of the profile with its thickness (t) at a given rib position determine the material cross section (A) of the upper and lower skin panels. The sum of the material at all rib positions leads to the minimum weight of all skins and stiffeners to withstand bending. Structure sizing for torsion and shear force are also taken from [7]. The leading and trailing edge devices of the secondary structure are considered to be similar for hybrid and conventional aircraft. Their masses are computed using the specific mass per area defined in [6].

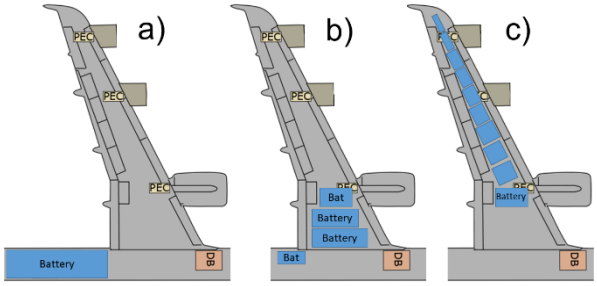

Figure 5 Change in Battery Position

The local impact of the span wise position of systems can be directly considered, as the sizing of the wing box is conducted at each rib station. The minimum wing mass is calculated iteratively by moving the battery from the fuselage into the wing, as shown in Figure 5. At each battery position, the length of electrical cables and thermal pipes are calculated and taken into account for the lift relief. The position of the electric fans and gas turbine are design variables in the overall optimization. The dimensions of pipes and cables depend on their length. They are output values of the models by the TRADE partners Nottingham and Mälardalen. Their initial values underlying the parameter studies in Chapter 4 are summarized in Table 4.

Table 4 Underlying Values of Cables and Pipes

Component	Length [m]	Diameter [m]	Mass / meter [kg/m]
AC cable 1	0.3	0.029	1.5
AC cable 2-3	0.3	0.026	1.3
DC cable 1	9.1	0.19	42.0
DC cable 2	21.4	0.17	36.2
DC cable 3	25.2	0.17	36.2
DC cable 4	0.3	0.39	188
Pipe 1-14	0.3 – 25.5	No input	14.7

A correction of non-optimum mass effects as manufacturing constraints is conducted in a final step.

3.3. Tail plane

Horizontal Tail Plane (HTP)

The statistical HTP mass (M_{HTP}) is computed as a function of the dive speed (V_D), sweep angle (Λ_{HTP}) and horizontal tail plane area (A_{HTP}). According to Torenbeek, factor k_{HTP} equals 1 for fixed stabilizers [5]. Λ_{HTP} and A_{HTP} are design variables in the MDAO environment. The aircraft description in the CPACS file provides their initial values.

$$M_{HTP} = A_{HTP} \cdot k_{HTP} \cdot f\left(\frac{A_{HTP}^{0.2} \cdot V_D}{\sqrt{\cos \Lambda_{HTP}}}\right) \quad (5)$$

Vertical Tail Plane (VTP)

The moment of the VTP shall compensate the moment occurring with OEI. Therefore, the lift generated by the tail plane ($F_{VTP,c}$) must equal the sum of thrust of the operative engine ($F_{T,eng,c}$) and drag of the inoperative engine ($F_{D,eng,c}$). As the lever arm of the inoperative engine is equal to the operative engine, the forces are

$$F_{eng,c} = F_{T,eng,c} + F_{D,eng,c} \quad (6)$$

$$F_{VTP,c} = \frac{F_{eng,c} \cdot y_{eng,c}}{x_{VTP}} \quad (7)$$

Hereby, the GT and e-fan drag is set to equal the values of cylinders with equal length and diameter [3].

The electro-hybrid propulsion is designed in a way that one gas turbine in combination with two e-fans generates sufficient thrust to comply with CS 25 [1]. In case of an inoperative gas turbine during take-off, the e-fans on the opposing wing half are shut down. Therefore, replacing the conventional gas turbine with electro-hybrid propulsion changes the necessary amount of VTP lift (Eqs. 8-9). Figure 6 illustrates the OEI scenario.

$$F_i = F_{T,i} + F_{D,i} \quad (8)$$

$$F_{VTP,h} = \frac{F_{GT} \cdot y_{GT} - F_{EF1} \cdot y_{EF1} - F_{EF2} \cdot y_{EF2}}{x_{VTP}} \quad (9)$$

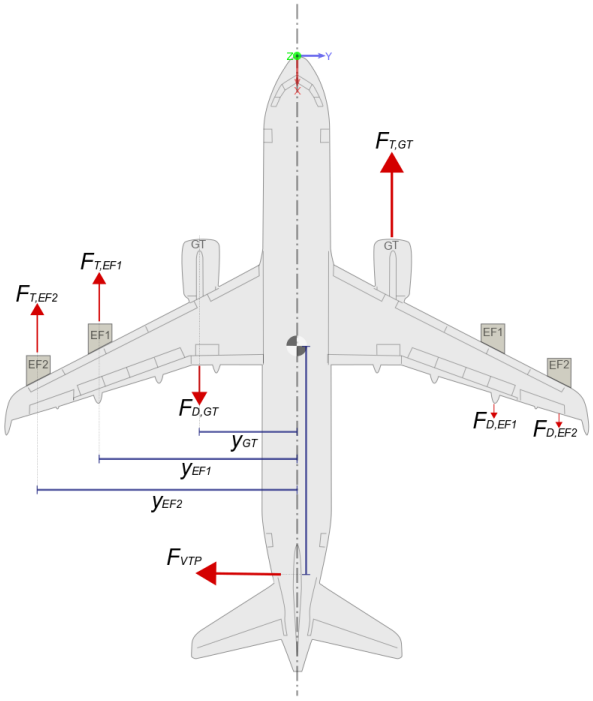

Figure 6 One Engine Inoperative

The surface of VTP is scaled using the definition of aerodynamic lift coefficient in Eq. 10.

$$c_L = \frac{F_{VTP,c}}{q \cdot A_{VTP,c}} = \frac{F_{VTP,h}}{q \cdot A_{VTP,h}} \quad (10)$$

$$A_{VTP,h} = \frac{F_{VTP,h}}{F_{VTP,c}} \cdot A_{VTP,c} \quad (11)$$

The mass calculation is conducted using Eq. 11. Similar to the HTP, the initial values taken from the CPACS file become design parameters within the MDAO environment.

$$M_{VTP,h} = A_{VTP,h} \cdot k_{VTP} \cdot f\left(\frac{A_{VTP,h}^{0.2} \cdot V_D}{\sqrt{\cos \Lambda_{VTP}}}\right) \quad (12)$$

Eq. 12 is solved assuming a constant lever arm of the VTP. The lever arm depends on the position of the overall aircraft center of gravity (CG), which depends on the VTP mass as well as the mass and position of EPS and thermal components. All vary during the conducted parametric studies and the multidisciplinary optimization. In future studies, the CG needs to be evaluated and the stability of the aircraft ensured.

4. Parameter Study

The parameter studies show the effect of changes in design parameters as well as inputs from other models.

A further outboard battery position is expected to yield a lighter primary structure. Therefore, the available volume between ribs and spars is filled with the battery. It is assumed, that the battery cells can be spread individually. A bulk factor of 0.8 accounts for unused space caused by the stiff and solid cell characteristics (battery is not “poured” into space).

Figure 7 shows the effect of the battery position on the wing structure mass. The rib number 0 is at the wing root while rib number 23 marks the wing tip. Markers a) to c) refer to the battery constellation shown in Figure 5.

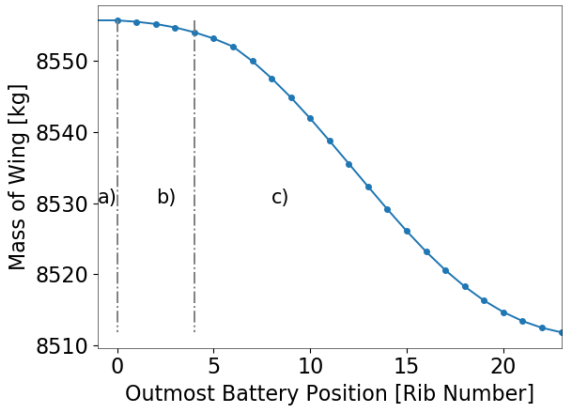

Figure 7 Mass Reduction due to Static Loads

The wing mass does not change while the battery is completely inside the fuselage (a)). In b) the battery is split between the fuselage and wing. The small lever arm of the inboard rib-volumes causes the gentle decline. The decline in mass correlates with the volume between ribs. The further outboard the smaller is the available volume. Hence, the mass drops less (c)). The reduction of structure mass reflects the reduced moment as result of the lift relief introduced in chapter 3.2.

As the position of battery directly influences the mass of installed pipes and cables, their mass needs to be regarded. The effects of the battery position on the pipe and cable mass is shown in Figure 8.

The high mass of the cable connecting the distribution board (DC cable 4) leads to a steep increase in cable and pipe mass. The maximum increase in cable mass is 12.8 times higher than the potential reduction of wing mass.

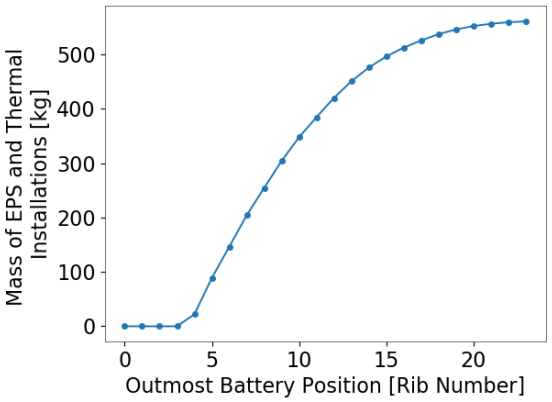

Figure 8 Change in Cable and Pipe Mass

The battery is positioned behind the wing box while it is inside the fuselage. Inside the wing, its span wise position is variable. In order to get the greatest relief with no cable mass penalty, the battery should be placed within the wing close to the root.

The tendency of the maximum take-off mass with different battery masses shows an almost linear trend (Figure 9). The structural relief of the primary wing structure becomes visible when a straight line is added (red dashed line).

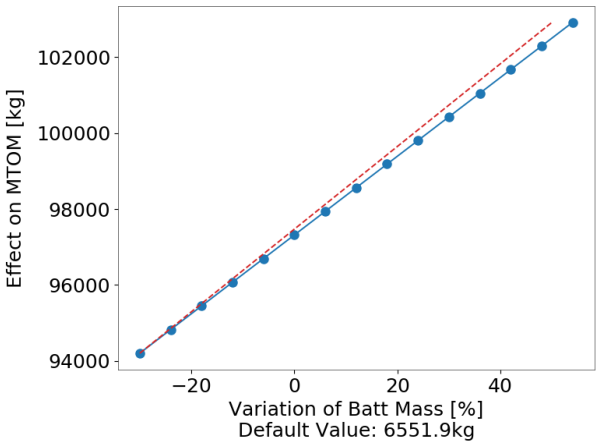

Figure 9 Trend of Maximum Take Off Mass under Varied Battery Mass

A change in wing area also changes the maximum take-off mass almost linearly. Judging from Figure 10, a small wing seems reasonable. A disadvantage of a small wing is the high velocity

needed to generate lift. This parameter is not constraint within the structure model. An overall optimization is most likely to yield a minimum area for realistic aircraft handling.

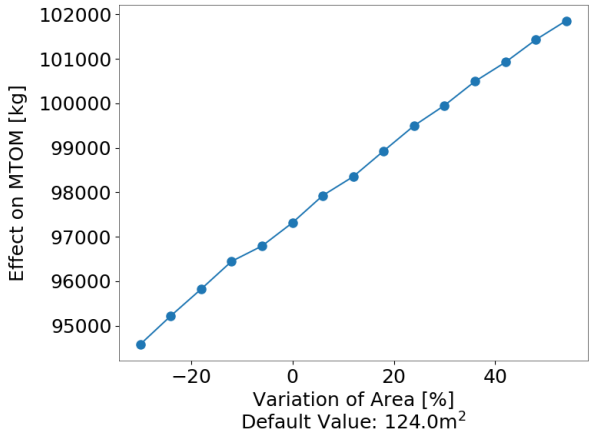

Figure 10 Effect of Wing Area Variation on MTOW

5. Conclusion

The steep increase in take-off mass shows that the desired lowering in structural mass is reduced strongly by the gain in the systems' mass. Hence the battery should be positioned completely within the wing at the root. The distance to the distribution board is the shortest in this position.

The variation of the wing area indicates that a small wing is preferable. This is caused by the very basic aerodynamic methods and the missing constraints due to aircraft operation.

The conducted studies include the structure model only. In the greater design environment, a mission model is closely linked and undertakes calculations, which are normally considered in the structural design. In addition, some parameters, such as the wing area and maximum necessary fuel mass, are design parameters, which were held constant when they were not the studied parameter. Changes in masses per meter of pipes and cables for different layouts were not considered. Therefore, it is worth mentioning that only tendencies of interdependencies were made visible.

6. Acknowledgements

The model was developed as part of the Clean Sky 2 Project TRADE, under grant agreement number 755458. The authors highly appreciate the collaboration with their Partners Xin Zhao, Smruti Sahoo, Dimitra Eirini Diamantidou, Mavroudis Kavvalos and Konstantinos Kyprianidis from Mälardalen University, Sweden, Sharmila Sumsurooah and Giorgio Valente from Nottingham University, UK, Jonatan Rantzer, Clément Coïc, and Michael Sielemann from Modelon, Sweden and Tobias Hecken from the German Aerospace Center DLR. The authors also thank Andreas Gobbin (TU Berlin) for the contribution of technology factors.

7. Literature

1. (2007) *Certification Specifications for Large Aeroplanes Amendment 3*. CS-25 Amd 3 Certification Specifications for Large Aeroplanes

2. European Commission Directorate-General for Research and Innovation (2011) *Flightpath 2050 Europe's Vision for Aviation*. Report of the High Level Group on Aviation Research, Luxembourg: European Union

3. Hucho W-H (2012) *Aerodynamik der stumpfen Körper*. Physikalische Grundlagen und Anwendungen in der Praxis, 2. Aufl. Vieweg+Teubner Verlag, Wiesbaden

4. IAA SciTech Forum (Hrsg) (2020) *Conceptual Design Studies of "Boosted Turbofan" Configuration for Short Range*. CleanSky2 LPA WP1.6.1.4 special session. IAA

5. Torenbeek E (1976) *Synthesis of subsonic airplane design*. An introduction to the preliminary design of subsonic general aviation and transport aircraft, with emphasis on layout, aerodynamic design, propulsion and performance. Delft University Press, [Delft]

6. Torenbeek E (1992) *Development and Application of a Comprehensive, Design-Sensitive Weight Prediction Method for Wind Structures of Transport Category Aircraft.* Report LR, Delft

7. Valente G, Sumsurooah, Hill CI (Hrsg) (2020) *Design Methodology and Parametric Design Study of the On-Board Electrical Power System for Hybrid Electric Aircraft Propulsion.*

8. Zhao X, Sahoo S, Kyprianidis K (Hrsg) (2019)
A Framework for Optimization of Hybrid Aircraft